Chemistry–A European Journal
Research Article
doi.org/10.1002/chem.202302758
Chemistry Europe
European Chemical Societies Publishing
www.chemeurj.org

Dimerization and Crowding in the Binding of Interleukin 8 to Dendritic Glycosaminoglycans as Artificial Proteoglycans

Jan-Niklas Dürig,[a] Christian Schulze,[b] Mathias Bosse,[b] Anja Penk,[b] Daniel Huster,[b] Sandro Keller,[c] and Jörg Rademann*[a]

The interactions of glycosaminoglycans (GAG) with proteins of the extracellular matrix govern and regulate complex physiological functions including cellular growth, immune response, and inflammation. Repetitive presentation of GAG binding motifs, as found in native proteoglycans, might enhance GAG-protein binding through multivalent interactions. Here, we report the chemical synthesis of dendritic GAG oligomers constructed of nonasulfated hyaluronan tetrasaccharides for investigating the binding of the protein chemokine interleukin 8 (IL-8) to artificial, well-defined proteoglycan architectures. Binding of mutant monomeric and native dimerizable IL-8 was investigated by NMR spectroscopy and isothermal titration calorimetry. Dendritic oligomerization of GAG increased the binding affinity of both monomeric and dimeric IL-8. Monomeric IL-8 bound to monomeric and dimeric GAG with K_D values of 7.3 and 0.108 μM, respectively. The effect was less pronounced for dimerizable wild-type IL-8, for which GAG dimerization improved the affinity from 34 to 5 nM. Binding of dimeric IL-8 to oligomeric GAG was limited by steric crowding effects, strongly reducing the affinity of subsequent binding events. In conclusion, the strongest effect of GAG oligomerization was the amplified binding of IL-8 monomers, which might concentrate monomeric protein in the extracellular matrix and thus promote protein dimerization under physiological conditions.

Introduction

Glycosaminoglycans (GAG) are complex sulfated polysaccharides of the extracellular matrix governing the translocation, mobility, and biological activity of numerous proteins within the extracellular space.[1] Among others, GAG binding of proteins have been found to mediate or inhibit receptor binding, trigger a chemotactic gradient,[1b,2] or protect proteins from degradation.[3] The architectures of high molecular weight GAG (>500 kDa), low-molecular-weight GAG (<500 kDa), and GAG oligosaccharides (<7 kDa)[4] are characterized by repeating disaccharide units that can bear sulfate residues, as found in heparin, chondroitin sulfate, and keratan sulfate. As the density of sulfate residues (i.e. the degree of sulfation) can vary throughout the polysaccharide, multiple different binding motifs are generated to modulate protein functionality.[5] Although hyaluronic acid is non-sulfated in its native form, chemically synthesized, highly sulfated hyaluronan oligosaccharides display at least equally strong binding to cytokines and growth factors as the naturally occurring heparin and, thus, are useful models for studying GAG-protein interactions.[6]

Recently, we have investigated the binding of defined sulfated GAG to a selection of ten representative GAG-binding proteins by biophysical and computational methods, which yielded several insights into GAG–protein binding.[7] One observation was that the binding affinity of highly sulfated tetra- or hexahyaluronans as exemplary GAG motifs to proteins was substantially enhanced through dimerization of the GAG motif. The effect was most pronounced for the protein interleukin 8 (IL-8), with a 400-fold increase in the binding affinity upon going from the monomeric to the dimeric nonasulfated tetrahyaluronan in a fluorescence polarization assay. Increased binding of dimeric GAG to IL-8 was also observed, although to a lesser extent, by isothermal titration calorimetry (ITC) as an orthogonal method.

As oligomerization of GAG motifs is typical both for the native polysaccharides of the extracellular matrix and for proteoglycan structures, we decided to synthesize and investigate a set of dendritic and linear oligomers of GAG binding sites as models for proteoglycan structure and for studying protein binding events. IL-8 was selected as an exemplary protein target in this study due to its well-described binding to various GAG. This chemokine has been reported to form homodimers, which might influence GAG binding as well.[8]

[a] Dr. J.-N. Dürig, Prof. Dr. J. Rademann
Institute of Pharmacy – Medicinal Chemistry
Freie Universität Berlin
Königin-Luise-Str. 2+4, 14195 Berlin (Germany)
Corresponding author
E-mail: joerg.rademann@fu-berlin.de

[b] Dr. C. Schulze, M. Bosse, Dr. A. Penk, Prof. Dr. D. Huster
Institute of Medical Physics and Biophysics
Leipzig University
Härtelstr. 16/18, 04107 Leipzig (Germany)

[c] Prof. Dr. S. Keller
Biophysics, Institute of Molecular Biosciences (IMB)
NAWI Graz, Field of Excellence BioHealth
BioTechMed-Graz, University of Graz
Humboldtstr. 50/III, 8010 Graz (Austria)

Supporting information for this article is available on the WWW under https://doi.org/10.1002/chem.202302758

Several different K_D values for the homodimerization of IL-8 have been determined, with variations supposedly resulting from the use of different binding assays, buffers, and methods.[8] ITC yielded dimerization constants in the low micromolar range (10–18 μM).[9] Although little is known about the concentration of IL-8 in the extracellular matrix, concentrations of IL-8 in serum are in the range of 1.7–3.1 pM,[10] suggesting that the protein should be present almost exclusively as a monomer under physiological conditions. Binding of naturally occurring sulfated GAG such as heparan or chondroitin sulfate enhances dimerization.[11]

The biological activity of IL-8 is also correlated with its monomer–dimer equilibrium. While the monomer has a higher receptor binding affinity, the dimer has a higher GAG binding affinity.[12] Furthermore, the dimer seems to be more stable and triggers further IL-8 multimerization, which increases its local concentration.[11c] Experiments with a strictly monomeric IL-8 mutant in comparison with wild-type IL-8 or a trapped dimer have indicated that the monomer recruits neutrophils at lower concentrations over a longer time period, whereas the dimer is able to recruit more neutrophils faster.[13]

In this study, we first used NMR spectroscopy to determine the binding sites of oligomeric GAG on monomeric and dimeric IL-8 and compared them with those of naturally occurring heparin hexasaccharide. Next, we used ITC to determine the binding affinities, thermodynamics, and stoichiometries of dendritic GAG for monomeric and dimeric IL-8. In particular, we aimed at identifying crowding effects and the role of multivalency, that is, the influence of the repetitive binding motif and its steric representation to the protein. Finally, a qualitative model was devised to explain the interplay of multivalency and crowding effects in the binding of oligomeric GAG to monomeric and dimeric IL-8.

Results and Discussion

Chemoenzymatic synthesis of di-, tri- and tetramerically presented nonasulfated hyaluronan tetrasaccharides

To investigate protein binding to dendritic oligomeric GAG, we decided to synthesize precisely defined molecules as opposed to the inhomogeneous polymeric structures found in native proteoglycans. Therefore, all linkers should resemble the same core structure (propane-1,3-diol) and the same attachment (triazole). Hence, propane-1,3-diol was deprotonated with sodium hydride and reacted with propargyl bromide to give the bivalent linker **1**. For the trivalent linker, the more stable 2-(hydroxymethyl)-2-methylpropane-1,3-diol rather than the less stable 2-(hydroxymethyl)propane-1,3-diol was chosen as starting molecule, with the assumption that the methyl group does not influence the binding behavior significantly. This reaction gave the propargylated triether **2**. As an equivalent of the propanediol in tetravalent form, pentaerythritol resembles the core structure best. From this, the tetravalent alkyne **3** was synthesized accordingly (Figure 1A).

The synthesis of the tetrasaccharide azide **4** followed the chemoenzymatic protocol established in our group.[14] In brief, digestion of high-molecular-weight hyaluronan with bovine testes hyaluronidase, yielded a mixture of di-, tetra- and hexasaccharides (HA-2, HA-4, and HA-6) which was separated by size exclusion chromatography (Bio-Gel P2-column extra fine 3.5x90 cm, 25% acetic acid, 5 psi). The reducing anomeric center of the tetrasaccharide was modified using the reagents chloro-dimethylimidazolium chloride (DMC) and sodium azide. The reaction furnished exclusively β-configured glycosyl azide **4**, as confirmed by ^{1}H NMR and the coupling constant of the respective anomeric proton ($J = 9.5$ Hz). **4** was coupled to the multivalent linkers in a 1:1 ratio of azide to alkyne (Figure 1B). The reaction catalyzed by copper sulfate reduced with sodium ascorbate, and tris((1-benzyl-4-triazolyl)methyl)amine (TBTA) was performed in degassed MeOH and water. Full conversion of the alkyne residues to the fully substituted bi-, tri-, and tetrameric products **6**, **8**, and **10** was monitored by HPLC-MS and high-resolution MS (Figures S1–S6). The structures of all products were confirmed by the assignment and integration of characteristic signals in ^{1}H and ^{13}C NMR spectra (Figures S7–S15). The overlay of spectra of starting materials **1** and **4** with the one of product **6** showed that the protons of the first sugar residue (I–H1 and I–H2) and the I–N-acetyl group were shifted downfield, while protons of the linker group and the signals of the other sugars remained unchanged, the terminal alkyne protons (2.42 ppm) disappeared and the triazole protons (8.24 ppm) were formed (Figure S16 in the Supporting Information). Subsequently, dendritic products **6**, **8**, and **10** were sulfated with an excess of SO_3·DMF complex. The reaction was conducted in dry DMF and products precipitated as sodium salts after the addition of sodium acetate in cold ethanol. The filter cake was dissolved in and extensively dialyzed (MWCO = 1 kDa) against deionized water. Lyophilization gave the final products **7**, **9**, and **11** (Figure 1C). Successful persulfation was confirmed by ^{1}H NMR spectroscopy (Figures S11, S13, and S15), since modification of an alcohol moiety with the electron-withdrawing sulfate group shifted all ^{1}H backbone signals of the oligosaccharides to lower field (Figure S17).[1b,7]

NMR studies of IL-8^{wt}

To map the IL-8 binding epitope of the dendritic GAG oligomers, NMR studies were conducted with wildtype IL-8 (IL-8^{wt}) at a concentration of 100 μM. ^{1}H-^{15}N HSQC spectra of fully ^{15}N-labeled IL-8^{wt} as a homodimer were acquired with increasing amounts of either heparin hexasaccharide or divalent **7**, trivalent **9**, and tetravalent **11** dendrimers of the nonasulfated hyaluronan-tetrasaccharide **5**. The NMR spectrum of IL-8^{wt}(1–77) showed chemical shift perturbations (CSP) upon addition of heparin dp6 and **9**. The weighted CSP at equimolar ratio of protein and ligand are shown in Figure 2. By adding heparin hexasaccharide to IL-8^{wt}, the weighted CSP changed most significantly near to or within the N-loop and the α-helical region (residues K25-I27 and N61-S77). Particularly the C-terminal α-helix including the strongest CSP for residue V66 and

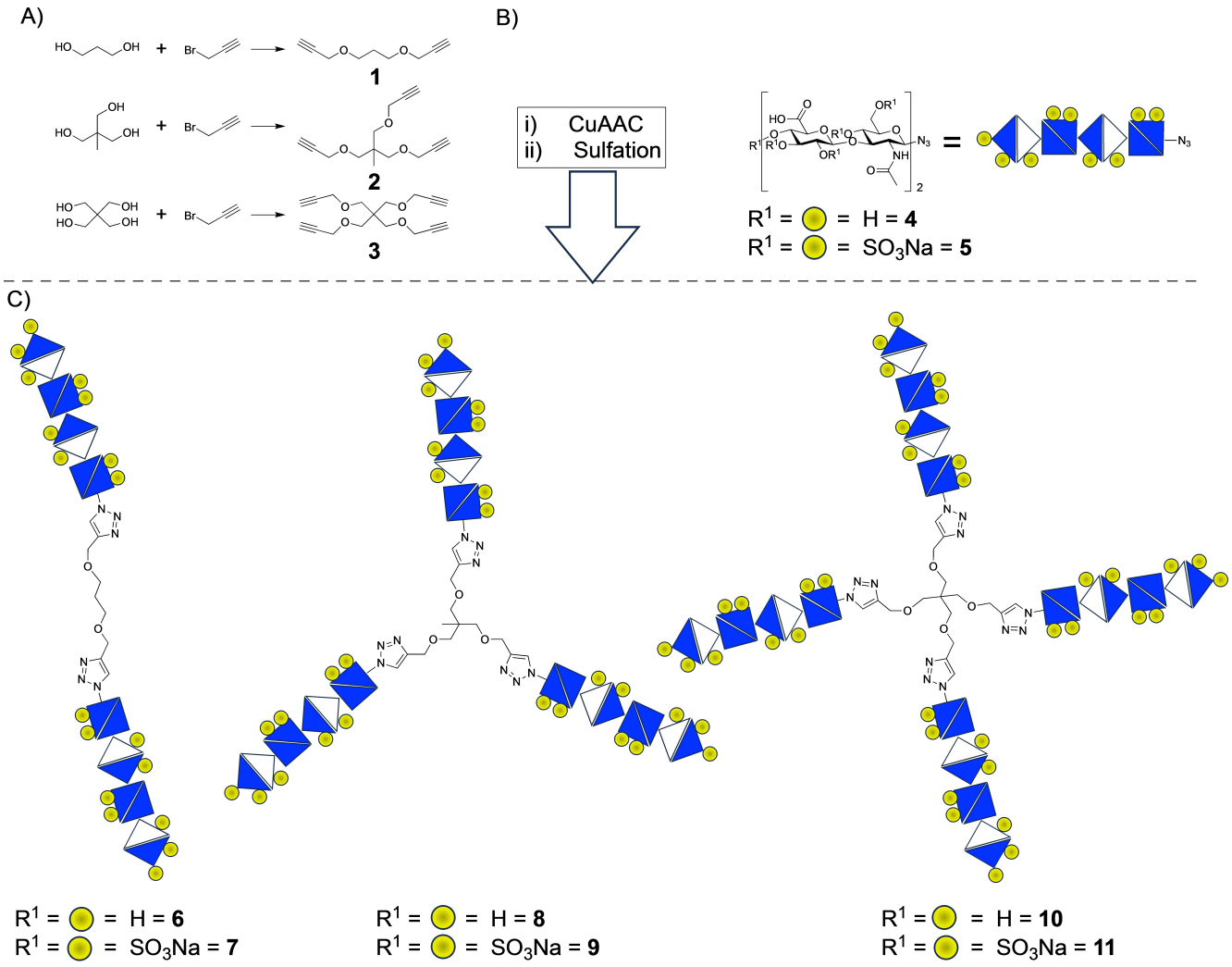

Figure 1. Synthesis of dendritic GAG-oligosaccharides. A) Synthesis of the multivalent alkyne linkers **1–3**. Reaction conditions: 1.5 equiv. NaH, 1.5 equiv. propargyl bromide per OH group, DMF, 58–71 % yield. B) Coupling of the tetrahyaluronan azide **4** (HA4-azide) to the alkyne linkers, followed by sulfation. Reaction conditions: i) TBTA, Na-ascorbate, $CuSO_4 \cdot 5H_2O$, degassed MeOH/H_2O (5 : 1). ii) SO_3·DMF, dry DMF. C) Schematic structures of compounds **6–11**.

A74, and residues H23 and K20 next to the N-loop were highly affected by binding of heparin hexasaccharide. Thus, the amino acids affected by the binding of heparin dp6 were the same as described for the interaction of IL-8 with heparin in different degrees of polymerization (2 to 26 sugar units)[14] as well as chondroitin and dermatan sulfate hexasaccharides.[6] For the trivalent **9** dendrimer, the same regions were affected (K20, F22, H23, and the C-terminal helix). While the C-terminal helix showed overall lower CSP at equimolar ratio of ligand **9** compared to the heparin, the N-terminal residues F22 and H23 showed higher CSP. Consequently, the synthesized trivalent GAG dendrimer **9** interacted with IL-8^{wt} by the same binding epitope as the heparin hexasaccharide, as well as other GAG.

By adding heparin hexasaccharide, the divalent **7**, trivalent **9** and tetravalent GAG dendrimer **11** to the protein, we observed a loss of signal intensity in the ^{1}H-^{15}N HSQC spectra, combined with an increased turbidity of the sample. After some incubation time, the sample solution became clear again and no visible aggregation of the protein was observable. This behavior is well known for the IL-8-GAG system and especially pronounced at high protein concentrations.[15a] In more detail, the NH spectral intensity in a 1D spectrum decreased by a factor of ~2 in the presence of heparin hexasaccharide and the trivalent GAG dendrimer **9** at equimolar concentrations compared to the spectra with IL-8^{wt} alone, while the divalent GAG oligosaccharide **7** lead to the intensity decrease about the factor 4 at equimolar concentrations. To counteract this signal loss, a 16-fold higher measuring time per spectrum would be necessary to obtain the same signal to noise ratio. However, the tetravalent GAG dendrimer **11** already decreased the signal intensity about the factor 6 by adding 20 μM ligand to the 100 μM protein solution (1:0.2). Hence, although we measured at 100 μM IL-8, a rather low protein concentration (by NMR standards), this loss of intensity by adding **7** and **11**, did not allow for meaningful titration spectra. This precluded the complete NMR titration experiments for the divalent **7** and tetravalent **11** proteoglycan toward IL-8^{wt}. The loss of signal intensity in the ^{1}H-^{15}N HSQC spectra indicated the formation of

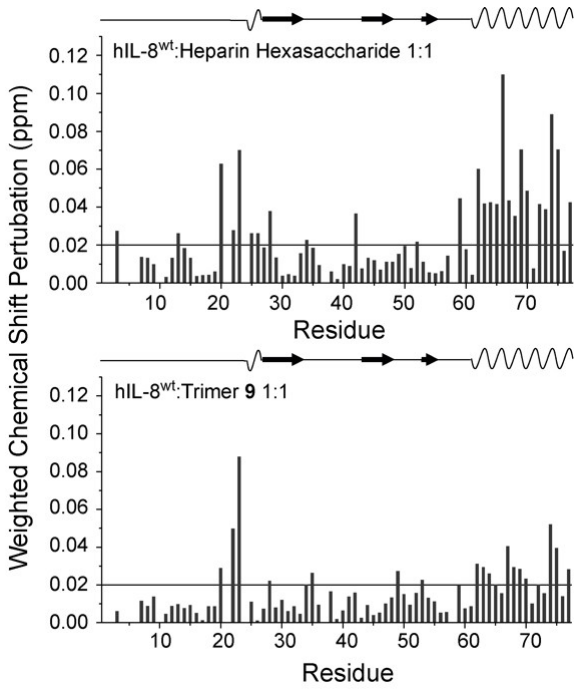

Figure 2. Calculated weighted chemical-shift perturbation (CSP) for the equimolar ^{1}H-^{15}N HSQC titration experiment of the heparin hexasaccharide (top) and the trimeric dendrimer **9** (bottom) towards IL-8^{wt}. The black line indicates the significance threshold of 0.02 ppm. Additionally, the secondary structure of IL-8^{wt} is shown on top of each graph (α-helical = waves, β-sheet regions = arrows).

high molecular weight structures induced by the ligands, as rather a complete loss of the signal was observed than line broadening. Taken together, the induction of large molecular structures or aggregates was most pronounced for the tetravalent dendrimer **11**, followed by divalent structure **7** and least for trivalent GAG dendrimer **9** and the linear heparin hexasaccharide. This may resemble the different three-dimensional structure of the synthesized proteoglycans. While the divalent **7** and tetravalent **11** proteoglycan are free to form linear oligomers, the trigonal structure of the trivalent GAG dendrimer **9** might prevent this.

The formation of oligomers of chemokines induced by GAG, depending of the GAG length and protein concentration has been already described in other studies.[16] However, it seems that the high concentration of sulfate groups in the synthesized dendrimers (4.5 per disaccharide unit compared to ~3 per disaccharide unit for heparin) promotes the effect of protein oligomerization.

Isothermal titration calorimetry

ITC was conducted to determine the thermodynamics and stoichiometry of the binding of monomeric and dimerizable, IL-8^{wt} to monomeric GAG **5** and to the dendritic GAG constructs **7**, **9**, and **11**. In a first series of experiments, 50 μM solutions of mono- and oligomeric GAG ("artificial proteoglycans") were titrated to 10, 20 or 40 μM solutions of wild-type, dimerization-competent IL-8^{wt} or mutated, monomeric IL-8 (IL-8^{mut}). The nonasulfated tetrahyaluronan **5**, the "GAG monomer", bound to IL-8^{wt} with a molar binding enthalpy of $\Delta H^{\circ} = -46\ kJ\,mol^{-1}$ and a molar entropy loss of $-T\Delta S^{\circ} = +3\ kJ\,mol^{-1}$, corresponding to a dissociation constant (K_D value) of 34 nM (Figure 3A).[7] The same experiment indicated a stoichiometry or binding ratio of 0.37 GAG molecules per protein monomer, that is, 2.7 IL-8 monomers per GAG. Binding of **5** to the mutated monomeric IL-8^{mut} displayed a similar binding enthalpy ($\Delta H^{\circ} = -48\ kJ\,mol^{-1}$) and stoichiometry (0.42, i.e., 2.4 proteins per GAG), but the entropy loss ($-T\Delta S^{\circ} = +29\ kJ\,mol^{-1}$) was much larger than for IL-8^{wt} (Figure 3B).

This significant reduction in entropy upon binding reflects the decreased degrees of freedom of the bound monomeric IL-8^{mut} proteins forming a complex with **5** and resulted in a K_D value of 7.3 μM, indicating that the binding affinity of the mutant was reduced more than 200-fold compared to the

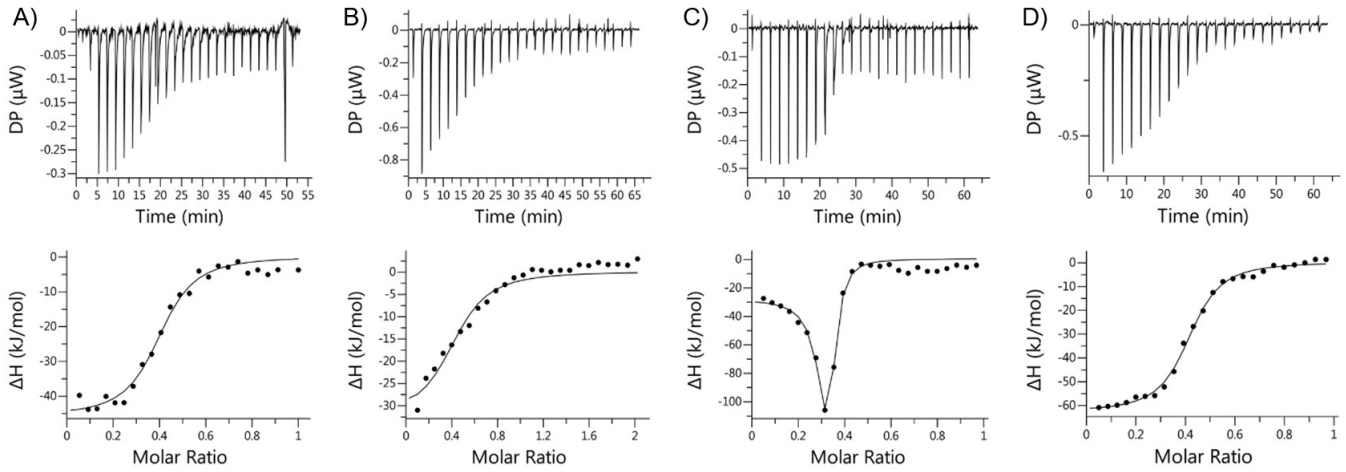

Figure 3. Thermograms (top) and isotherms (bottom) of ITC experiments. A) 50 μM solution of monomeric GAG tetrasaccharide **5** to a 10 μM solution of IL-8^{wt} (taken from Köhling et al.[7], CC BY-NC 3.0). B) 200 μM solution of monomeric GAG tetrasaccharide **5** to a 40 μM solution of IL-8^{mut}. C) 50 μM solution of dimeric GAG tetrasaccharide **7** to a 10 μM solution of IL-8^{wt}. D) 50 μM solution of dimeric GAG **7** to a 10 μM solution of IL-8^{mut}.

dimerizable wildtype protein. The much smaller entropy loss during the binding of IL-8^{wt} to GAG **5** might indicate that this protein was already dimerized in the solution.

Binding isotherms of the dimeric, trimeric, and tetrameric GAG dendrimers **7**, **9**, and **11** titrated to dimeric wild-type IL-8^{wt} (Figure 3C) deviated strongly from the sigmoidal curve typical of simple binding reactions (see Figure 3C for **7** and Figure S19 for **9** and **11**). For GAG-dimer **7**, for example, the negative heat of reaction (normalized to the molar amount of injected GAG) started at a low level at $-30\ kJ\,mol^{-1}$ during the first stage of the titration but then strongly increased in magnitude to $-120\ kJ\,mol^{-1}$ at a molar ratio of 3.4 IL-8 monomers per GAG dimer **7** or 1.7 IL-8 monomers per GAG monomer (Figure 3C). After this point, the heat of reaction steeply decreased in magnitude to approach baseline levels. Fitting the upward part of the binding isotherm yielded an apparent dissociation constant of 55 nM. Binding isotherms, thermodynamic contributions, affinities, and stoichiometries per GAG monomer were similar for GAG dimer **7**, trimer **9**, and tetramer **11** (Figure S19, Table 1). Oligomerization of GAG in **7**, **9**, and **11** did not increase the apparent affinities. The results of the ITC experiments with oligomeric GAG and IL-8^{wt} demanded a biophysical explanation. The obtained binding isotherms could not be fitted assuming a single set of binding sites. This suggested the occurrence of several subsequent binding events.

Next, the binding of oligomeric GAG with the mutated monomeric IL-8^{mut}, which is not able to form homodimers, was investigated. All binding isotherms measured for oligomeric GAG and monomeric IL-8^{mut} displayed canonical, sigmoidal shapes and, thus, could be fitted in terms of a simple, one-to-one binding model (Figures 3D and S18). Apparently, only dimerizable IL-8^{wt} but not monomeric IL-8^{mut} gave rise to the noncanonical binding isotherms observed above. Therefore, we suspected that molecular crowding during the binding of IL-8 dimers might occur in the early stages of ITC experiments with the dimerizing wildtype protein. Specifically, many protein dimers bind simultaneously to the few oligomeric GAG ligands present at the beginning of a titration. This crowding effect might be less pronounced for monomeric IL-8^{mut}, which is smaller and, thus, has less steric demand.

To test this crowding hypothesis, we conducted reverse titrations. In these experiments, a high concentration of IL-8^{wt} (510 and 255 μM, respectively) was titrated to a 15 μM solution of the multimeric GAG ligands **7** or **11** (Figures 4 and S20). These conditions generate a strong excess of GAG ligand at the beginning of the experiment, thus avoiding molecular crowding. The performed experiments resulted in binding isotherms displaying two consecutive binding events between IL-8 and oligomeric GAG **7** and **9**. Importantly, both global and local fits confirmed that binding proceeded in two steps differing in

Table 1. Thermodynamic parameters, dissociation constants and stoichiometry of the GAG constructs' binding to IL-8 determined by ITC.

Binding	IL-8 wild-type				IL-8 mutant			
parameter[a]	Monomer **5**[b]	Dimer **7**[c]	Trimer **9**[c]	Tetramer **11**[c]	Monomer **5**	Dimer **7**	Trimer **9**	Tetramer **11**
$\Delta G°$ [kJ mol^{-1}]	−42.7 ± 0.1	−41.6 ± 0.9	−39.2 ± 0.1	−44.2 ± 0.7	−29.4 ± 0.2	−39.8 ± 0.1	−38.4 ± 0.3	−39.3 ± 1
$\Delta H°$ [kJ mol^{-1}]	−45.8 ± 3.3	−292 ± 43	−176.5 ± 3.5	−327 ± 8	−48.1 ± 1.7	−63.4 ± 0.3	−93.4 ± 4.1	−117 ± 2
$-T\Delta S°$ [kJ mol^{-1}]	3.1 ± 3.1	250 ± 44	137.5 ± 3.5	283 ± 7	29.4 ± 0.2	23.7 ± 0.5	55.1 ± 3.8	77.9 ± 1.1
K_D [nM]	34.2 ± 2.0	55.9 ± 19	138.5 ± 7.5	19.4 ± 5	7295 ± 365	108 ± 17.6	195 ± 22	144 ± 54
n	0.37 ± 0.04	0.29 ± 0.008	0.25 ± 0.03	0.15 ± 0.02	0.42 ± 0.003	0.40 ± 0.003	0.33 ± 0.04	0.24 ± 0.0005

[a] ΔG = free energy of binding (Gibb's energy), ΔH = binding enthalpy, $-T\Delta S$ = negative entropic contribution, K_D = dissociation constants, n = binding stoichiometry of the GAG construct per protein monomer. [b] Taken from Köhling et al.[7] [c] One-to-one binding model fitted to the upward curve of the binding isotherm.

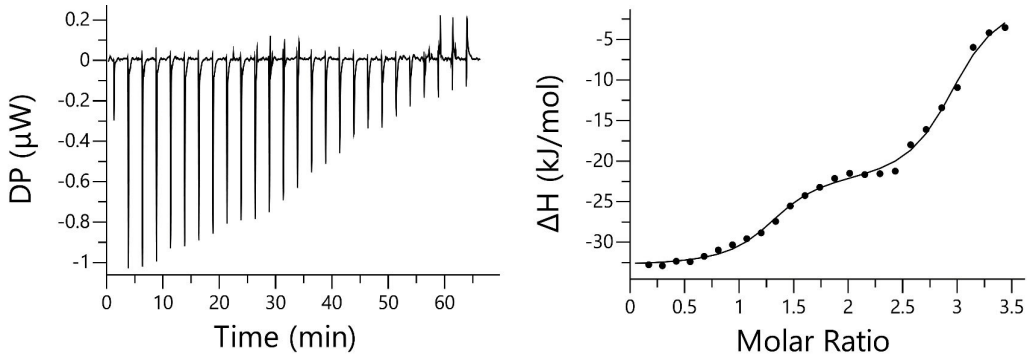

Figure 4. Reversed titration of IL-8^{wt} (255 μM) into a solution of dimeric GAG **7** (15 μM). Left: Thermogram. Right: Binding isotherm.

binding enthalpy and affinity. Thus, we analyzed these data in terms of a model assuming two sequential binding events (Table 2).

Accordingly, binding of IL-8 to **7** and **11** comprised a high-affinity binding step with K_D values 5 and 9 nM, respectively, driven by enthalpy and opposed by a strong entropic loss. This high-affinity binding event might reflect the uncrowded binding of one IL-8 dimer to one GAG oligomer ($n_1 = 2.7$ and 5.8). The second, low-affinity binding event displayed K_D values of 2.3 and 5.2 μM with a much smaller enthalpic contribution and entropic loss and a stoichiometry of $n_2 = 2.4$ for the GAG tetramer **11**. The entropic contribution was even negative for the GAG dimer **7** ($-T\Delta S_1 = -19\ kJ\,mol^{-1}$). The reduced binding affinity in the second binding event might result from the unfavorable, "crowded" secondary binding of IL-8 dimers to the GAG oligomers, possibly accompanied by the dissociation of IL-8 dimers into monomers and monomer binding to the GAG constructs.

Conclusions

We have synthesized a set of oligomeric GAG structures and investigated the binding of these dendritic architectures to monomeric and dimeric IL-8 proteins. NMR spectroscopy revealed that the monomeric GAG motif nonasulfotetrahyaluronan **5** and the trimeric GAG **9** occupy the same binding sites at IL-8 as the native GAG heparan sulfate. As the binding epitopes for monomeric and dimeric IL-8 do not differ or vary between different GAG-types,[6,15a] this finding implies that all investigated systems show the same binding site. The monomeric, non-dimerizable IL-8 mutant displayed a strong multivalency effect in the ITC titration of IL-8 monomer to a solution of GAG (Figure 3B and D). The binding affinity of monomeric IL-8^{mut} was improved from a K_D value of 7.3 μM with monomeric GAG **5** to 110 nM with dimeric GAG **7**. No further increase in affinity of IL-8 monomer was observed with trimeric and tetrameric GAG **9** and **11**. This finding suggests that the multimerization of GAG binding sites under physiological conditions is essential for the recruitment of monomeric IL-8 (Figure 5, top).

By contrast, the apparent binding affinities of wild-type dimeric IL-8 added to GAG did not increase from monomeric GAG **5** to dendritic GAG dimer **7**, GAG trimer **9**, and GAG-tetramer **11**. Binding isotherms of IL-8^{wt} with dendritic GAG oligomers **7**, **9**, and **11** deviated strongly from canonical sigmoidal curves. Reverse ITC titrations of GAG-oligomers **7** and **11** were conducted to rationalize the non-sigmoidal binding isotherms, revealing a multi-step binding event that could be fitted by assuming two independent sets of binding sites. Interpretation of the data suggested a first high-affinity binding event of IL-8 dimer to the GAG oligomer with K_D values of 5 and 9 nM, respectively. Secondary binding of IL-8 dimer or monomer to the GAG-oligomers occurred with low-micromolar affinity. The reduced affinity of the second binding can be rationalized as the result of a crowding effect. Whereas the first IL-8 dimer has free access to a GAG ligand and can undergo high-affinity binding, the binding of the second IL-8 dimer to a GAG-ligand suffers from steric hindrance (Figure 5, middle). Alternatively, steric hindrance might favor or allow monomer binding only, consuming additional energy for the dissociation of the IL-8 dimer. The crowding effect can rationalize the non-sigmoidal binding isotherms observed for the addition of GAG oligomers to a solution of IL-8 (Figure 5, bottom). In the beginning of this experiment, the excess of IL-8 over GAG oligomer is high, resulting in the reduced binding energy observed in the binding isotherm.

In summary, binding of the protein IL-8 to the synthetic oligomeric GAG structures displayed strong differences compared to binding of a monomeric GAG ligand. The affinity of dimeric GAG **7** was strongly enhanced, both in the primary binding event with IL-8^{wt} and, even more, with monomeric IL-8^{mut}. These observations were in agreement with the results of computational studies considering the binding of non-asulfotetrahyaluranes to IL-8 monomer and dimer.[7] The affinity enhancement through a multivalency effect was limited,

Table 2. Binding stoichiometry for the two consecutive binding events of the reverse titration (n^1 and n^2) with IL-8^{wt}. The intermediate plateau was calculated as the mean of n^1 and n^2 and the top plateau was calculated by addition of intermediate plateau and n^2.

Binding parameter[a]	Dimer **7**	Tetramer **11**
ΔG_1 [kJ mol^{-1}]	−47.6 ± 0.7	−46.0 ± 0.1
ΔH_1 [kJ mol^{-1}]	−76.6 ± 2.6	−210 ± 14
$-T\Delta S_1$ [kJ mol^{-1}]	29.1 ± 2.0	164 ± 14
K_{D1} [nM]	4.9 ± 1.3	8.8 ± 2.8
n^1	2.7 ± 0.2	5.8 ± 0.05
ΔG_2 [kJ mol^{-1}]	−32.9 ± 1.8	−30.3 ± 0.7
ΔH_2 [kJ mol^{-1}]	−13.9 ± 1.7	−35.4 ± 1.6
$-T\Delta S_2$ [kJ mol^{-1}]	−19.0 ± 3.5	5.1 ± 0.9
K_{D2} [nM]	2250 ± 1400	5240 ± 1400
n^2	2.1 ± 0.17	2.4 ± 0.24

[a] ΔG = free energy of binding (Gibb's energy), ΔH = binding enthalpy, $-T\Delta S$ = negative entropic contribution, K_D = Dissociation constants, n = binding stoichiometry of the protein monomer per GAG construct.

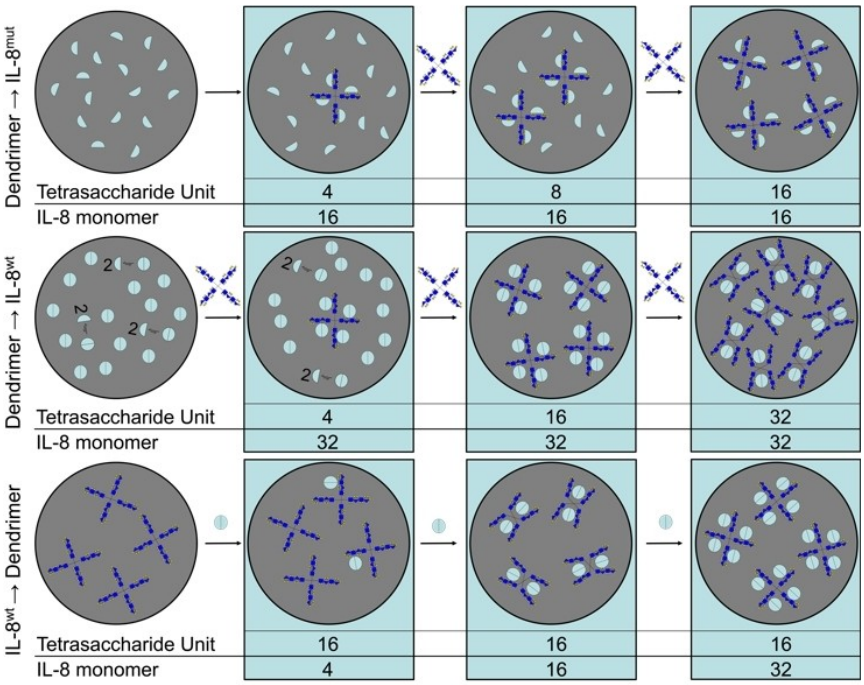

Figure 5. Schematic depiction of the proposed binding models. Top: The addition of the tetrameric GAG-dendrimer **11** to monomeric IL-8^{mut} resulted in sigmoidal binding isotherms that could be interpreted by the one-to-one binding model and a stoichiometry of about four proteins per GAG tetramer **11**. Middle: Titration of **11** to dimerizable IL-8^{wt} yielded noncanonical binding isotherms due to crowding and a stoichiometry of 6.7 per GAG tetramer **11**. Further addition of protein led to the binding of about four protein monomers per GAG tetramer. Bottom: Reversed titration of dimeric IL-8^{wt} to tetrameric GAG-dendrimer **11** revealed binding isotherms that were interpreted as two subsequent binding events, one with high affinity and a stoichiometry of 4–6 protein monomers per GAG tetramer and a second with low affinity due to crowding.

however, by a crowding effect that restricted the affinity of IL-8^{wt} but also that of monomeric mutant IL-8. Considering the low *in-vivo* concentrations of cytokines such as IL-8 under physiological conditions, the observed strong $>$60-fold affinity enhancement of monomeric IL-8 with oligomeric GAG seems to be most relevant for the maintenance and availability of this cytokine in the extracellular matrix.

Experimental Section

Protein expression: The 77 amino acid–containing human IL-8 (1-77) wild-type (IL-8^{wt}) was expressed, purified and refolded as previously described.[6] To form the monomeric version of IL-8 (1-77) (IL-8^{mut}), two amino acids (V32 and E34) located in the dimerization interface of IL-8^{wt} were mutated to proline by using mutagenesis PCR analogously to Joseph et al. for the 1–72 variant of IL-8.[17] Subsequently, the protocol of IL-8^{wt} was applied for IL-8^{mut}. For both proteins, the purity and molecular mass were confirmed using MALDI-MS. Additionally, the dimerization behavior was checked for IL-8^{wt} and IL-8^{mut} using size-exclusion chromatography using the Superdex® 200 10/30 GL column (Merck) and DOSY NMR (data not shown). NMR titration were performed with ^{15}N labeled IL-8^{wt} in 20 mM sodium phosphate, 50 mM sodium chloride and pH 7, while ITC was performed with unlabeled protein in PBS, as already described for other sulfated hyaluronan-derivatives.[7]

NMR titration of IL-8^{wt}: ^{1}H-^{15}N HSQC titration experiments were recorded on a Bruker Avance III 600 MHz spectrometer (Bruker BioSpin GmbH) equipped with 5 mm inverse triple resonance probe with z-gradient. NMR samples contained 100 μM fully ^{15}N-labeled IL-8^{wt} including 10% D_2O and 4 μM TSP for referencing and were measured at 30 °C.[18] For data acquisition and processing Topspin™ version 3.5 was used. For the analysis of the chemical shift perturbation (CSP) the software NMRFAM-Sparky was used.[19] During titration experiments, increasing amounts of heparin hexasaccharide or the respective artificial proteoglycan using a stem solution of 5 mM were added to the protein with 100 μM concentration. After each titration step, a ^{1}H-^{15}N fast HSQC spectrum, with a watergate 3–9-19 water suppression and a globally optimized alternating phase rectangular pulse (GARP) with a 90° pulse of 240 μs for ^{15}N decoupling was acquired.[20] In total 32, scans per increment were acquired to sample a spectral width of 25 ppm in the indirect dimension using 64 complex data points. Subsequently, the pH value of the measured solution was checked to confirm constant values during the experiments. By using the following equation, the weighted chemical shift change for each NH signal of the IL-8 backbone was calculated, where δ represents the CSP:

$$\Delta\delta(^{1}\mathrm{H},^{15}\mathrm{N}) = \sqrt{(\delta_{\mathrm{H}})^2 + (\delta_{\mathrm{N}}/5)^2}$$

Isothermal titration calorimetry: ITC was carried out in duplicates on a MicroCal PEAQ-ITC from Malvern Panalytical. While the data for 9 s-HA4-N_3 towards IL-8^{wt} titration and experimental conditions (PBS buffer, titration parameters) were adapted from our previous publication[7], concentrations for its titration towards IL-8^{mut} had to be adjusted (200 μM GAG towards 40 μM IL-8^{mut}). Each experiment consisted of 25 injections of 1.5 μL. For the dendritic molecules, the following concentrations were used:

Dendritic molecule	**7** [μM]	**9** [μM]	**11** [μM]
IL-8^{wt}/IL-8^{mut} [μM]	10\50	20\100	20\100
IL-8^{wt} (reversed titration) [μM]	255\15	n/a	510\15

Control experiments were performed and adjusted for in the MicroCal PEAQ-ITC Analysis Software:

	Cell					
Syringe	Buffer	IL-8^{wt} [μM]	IL-8^{mut} [μM]	**7** [μM]	**9** [μM]	**11** [μM]
buffer	1/1	10/20	10/20	15	n/a	15
	Syringe					
Cell	Buffer	IL-8^{wt} [μM]	IL-8^{mut} [μM]	**7** [μM]	**9** [μM]	**11** [μM]
buffer	1/1	255/510	n/a	50	100	50

Chemical synthesis: All starting materials for chemical synthesis were purchased from Sigma, VWR or abcr and were used without further purification. All experiments were performed under argon. Medium-pressure liquid chromatography (MPLC) was conducted with Biotage Isolera Spektra One and pre-packed flash chromatography cartridges from Biotage. Separation of non-sulfated hyaluronan derivatives was achieved using high performance liquid chromatography (HPLC) on an Agilent 1260 infinity system that was equipped with a C_{18} column from Machery–Nagel (Nucleodur, C18 Htec, 32.0×250 mm, 5.0 μM, 110 Å). Sulfated hyaluronan derivatives were dialyzed using Dialysis membrane Spectra/Por Biotech CE MWCO 100–500 (cellulose ester) or Spectra/Por 7 MWCO 1000 (regenerated cellulose) depending on molecular weight, which should be at least double the amount of the molecular-weight cut-off (MWCO). High-resolution mass spectrometry (HRMS) analyses were performed with Agilent 6550 iFunnel Q-TOF LC/MS (ESI–TOF, 10 μL min^{-1}, 1.0 bar, 4 kV). NMR experiments were conducted on JEOL ECX 400, JEOL ECZ 600 and Bruker AVANCE 700 instruments, using $CDCl_3$ (D, 99.8 %) and D_2O (99.9 %) as solvents. Chemical shifts are reported relative to the chemical shift of tetramethyl silane (0 ppm) in parts per million (ppm). Spectra are calibrated with respect to the solvent peaks.

1,3-Bis-(prop-2-yn-1-yloxy)-propane 1: Propane-1,3-diol (10 mmol, 0.7 mL) was dissolved in dry DMF (0.3 M) at 0 °C. Sodium hydride (60 % dispersion in mineral oil, 30 mmol, 1.2 g) was added, followed by propargyl bromide (80 wt% solution in toluene, 30 mmol, 3.3 mL) 15 min later. The reaction stirred at room temperature overnight. Access of sodium hydride was quenched by addition of methanol. All solvent was removed in vacuum, the residue taken up in ethyl acetate (100 mL) and washed with brine (100 mL). After drying the organic layer over $MgSO_4$ and removal of the solvent, the crude mixture was purified by MPLC (ethyl acetate in hexane, 0–5 %) and gave the final product as pale-yellow oil **1** (958.8 mg, 6.3 mmol). ^{1}H NMR (400 MHz, $CDCl_3$): $\delta = 4.14$ (d, $J = 2.4$ Hz, 4H), 3.61 (t, $J = 6.3$ Hz, 4H), 2.42 (t, $J = 2.4$ Hz, 2H), 1.89 (q, $J = 6.3$ Hz, 2H,) ppm. ^{13}C NMR (101 MHz, $CDCl_3$): $\delta = 80.00$, 74.34, 67.14, 58.30, 29.88 ppm. HRMS (ESI) calculated for $C_9H_{13}O_2^+$: 153.0910 Da $[M+H^+]^+$; found: 153.0911 *m/z*.

3-[2,2-Bis(prop-2-ynyl-oxymethyl)propyloxy]prop-1-yne 2: 2-(Hydroxymethyl)-2-methylpropane-1,3-diol (trimethylolethane; 1.0 mmol, 120.15 mg) was dissolved in dry DMF (0.3 M) at 0 °C and sodium hydride (60 % dispersion in mineral oil, 4.5 mmol, 180 mg) added. After 15 min. propargyl bromide (4.5 mmol, 501.2 μL) was added and the reaction mixture stirred overnight. After quenching the excess NaH with methanol, all solvents were removed in vacuum. The crude mixture was dissolved in ethyl acetate and washed with brine. Purification by MPLC (ethyl acetate in hexane, 0–10 %) gave the final product **2** as slight yellow viscous oil (140.6 mg, 58 %). ^{1}H NMR (400 MHz, $CDCl_3$): $\delta = 4.12$ (d, $J = 2.4$ Hz, 6H), 3.40 (s, 6H), 2.40 (t, $J = 2.4$ Hz, 3H), 0.97 (s, 3H) ppm. ^{13}C NMR (101 MHz, $CDCl_3$): $\delta = 80.23$, 74.17, 72.85, 58.81, 40.47, 17.48 ppm. HRMS (ESI) calculated for $C_{14}H_{19}O_3^+$: 235.1329 Da $[M+H^+]^+$; found: 235.1333 *m/z*.

Tetrakis(2-propynyloxymethyl)methane 3: 2,2-Bis(hydroxymethyl)-propane-1,3-diol (pentaerythritol; 1 mmol, 136.2 mg) was dissolved in dry DMF (0.3 M) at 0 °C. Sodium hydride (60 % dispersion in mineral oil, 6 mmol, 240 mg) was added, followed by propargyl bromide (80 wt% solution in toluene, 6 mmol, 668.3 μL) after 15 min. The reaction was allowed to come to room temperature and stirred overnight. Access sodium hydride was quenched by addition of methanol. The solvents were removed in vacuum. After taking the residue up in ethyl acetate (20 mL) and washing with brine (20 mL), the organic layer was dried over $MgSO_4$ and the solvent removed in vacuum. The crude mixture was purified by MPLC using a mixture of ethyl acetate in hexane (0–10 %) to yield the final product as a slight yellow solid (186 mg, 65 %). ^{1}H NMR (400 MHz, $CDCl_3$): $\delta = 4.12$ (d, $J = 2.4$ Hz, 8H), 3.53 (s, 8H), 2.40 (t, $J = 2.3$ Hz, 4H) ppm. ^{13}C NMR (101 MHz, $CDCl_3$): $\delta = 80.17$, 74.24, 69.17, 58.86, 44.91 ppm. HRMS (ESI) calculated for $C_{17}H_{21}O_4^+$: 289.1434 Da $[M+H^+]^+$; found: 289.1436 *m/z*.

Tetrahyaluronan dimer (HA4 dimer): 1,3-bis(β-D–glucopyranuronyl-(1→3)-β-D-2-acetamido-2-deoxyglucopyranosyl-(1→4)-β-D–glucopyranuronyl-(1→3)-β-D-2-acetamido-2-deoxyglucopyranosyl-(1,2,3-triazol-4-yl))methoxy-propane 6. 1,3-Bis(prop-2-yn-1-yloxy)-propane **1** (25 μmol, 3.8 mg), tetrahyaluronan azide **4** (50 μmol, 40 mg) and TBTA (1.8 μmol, 0.9 mg) was dissolved in dry degassed methanol (0.01 M). A solution of copper sulfate pentahydrate (2.5 μmol, 0.6 mg) in degassed H_2O (0.5 mL) was added followed by sodium ascorbate (5 μmol, 1 mg). The reaction was monitored via LCMS and additional sodium ascorbate added until no monosubstituted intermediate product was detectable. The solvent was removed in vacuum and the crude mixture purified first by size-exclusion chromatography (Sephadex G-10, H_2O) and secondly by HPLC (C-18, isocratic 95:5 H_2O (+0.1 %TFA)/MeCN (+0.1 %TFA) for 12 min to 50:50 in 20 min). Freeze-drying gave the final product **6** in a quantitative yield (43.7 mg) as a colorless powder. ^{1}H NMR (700 MHz, D_2O): $\delta = 8.24$ (s, 2H, triazole-H), 5.88 (d, $J = 9.5$ Hz, 2H, I–H1), 4.63-4.42 (m, 10H), 4.05-3.77 (m, 20H), 3.67-3.35 (m, 16H), 2.00 (s, 6H, I-NHAc), 1.87-1.83 (m, 2H, 2′-CH_2), 1.77 (s, 6H, III-NHAc) ppm. ^{13}C NMR (126 MHz, D_2O): $\delta = 174.93$, 174.20, 172.23, 171.25, 144.72, 124.07, 103.13, 102.80, 101.38, 86.36, 82.82, 82.23, 80.32, 78.74, 75.53, 75.23, 74.47, 73.85, 73.62, 72.62, 72.26, 71.31, 68.43, 68.09, 66.99, 62.82, 60.66, 54.39, 28.85, 22.56, 21.89 ppm. HRMS (ESI) calculated for $C_{65}H_{97}N_{10}O_{46}^-$: 1753.5564 Da $[M\text{-}H^+]^-$; found: 1753.5535 *m/z*.

Octadeca-sulfo tetrahyaluronan dimer (18 s-HA4 dimer): 1,3-bis(2,3,4,6-tetra-*O*-sulfo-β-D–glucopyranuronyl-(1→3)-4,6-di-*O*-sulfo-β-D-2-acetamido-2-deoxyglucopyranosyl-(1→4)-2,3,4,6-tetra-*O*-sulfo-β-D–glucopyranuronyl-(1→3)-4,6-di-*O*-sulfo-β-D-2-acetamido-2-deoxyglucopyranosyl-(1,2,3-triazol-4-yl))methoxypropane 7. Tetrahyaluronan dimer **6** (17 mg, 9.7 μM) was dissolved in dry DMF (0.024 M) and sulfur trioxide DMF complex (0.7 mmol, 111.2 mg) was added. After 14 h, additional SO_3·DMF (0.35 mmol, 55.6 mg) was added to ensure sulfation of all hydroxy groups. Two hours later, the final product was precipitated as a sodium salt by addition of sodium acetate (2 mmol, 171,9 mg) in cold ethanol (0.05 M). The filter cake was dissolved in and dialyzed (MWCO = 1000 Da) against deionized water. Lyophilization furnished the final product **7** as a colorless solid (25.1 mg, 71 %). ^{1}H NMR (700 MHz, D_2O): $\delta = 8.22$ (s, 2H, triazole-H), 6.01 (d, $J = 9.8$ Hz, 2H, I–H1), 5.19 (d, $J = 4.1$ Hz, 2H), 5.04–4.99 (m, 6H), 4.87–4.81 (m,

5H), 4.61–4.47 (m, 13H), 4.40–4.36 (m, 7H), 4.30–4.23 (m, 5H), 4.22–4.14 (m, 8H), 3.89–3.81 (m, 5H), 3.60 (t, $J=6.4$ Hz, 5H), 2.10 (s, 6H, I-NHAc), 1.83 (s, 6H, III-NHAc) ppm. ^{13}C NMR (126 MHz, D_2O): $\delta=$ 174.45, 174.34, 172.19, 171.88, 144.25, 124.22, 100.59, 99.83, 99.36, 85.60, 86.36, 82.82, 82.23, 80.32, 78.74, 75.53, 75.23, 74.47, 73.85, 73.62, 72.62, 72.26, 71.31, 68.43, 68.09, 66.99, 62.82, 60.66, 54.39, 28.59, 22.72, 22.05 ppm.

Tetrahyaluronan trimer, (HA4 trimer): 1,3-[2-methyl-2-(β-D–glucopyranuronyl-(1→3)-β-D-2-acetamido-2-deoxyglucopyranosyl-(1→4)-β-D–glucopyranuronyl-(1→3)-β-D-2-acetamido-2-deoxyglucopyranosyl-(1,2,3-triazol-4-yl))methoxymethyl]-bis(β-D–glucopyranuronyl-(1→3)-β-D-2-acetamido-2-deoxyglucopyranosyl-(1→4)-β-D–glucopyranuronyl-(1→3)-β-D-2-acetamido-2-deoxyglucopyranosyl-(1,2,3-triazol-4-yl))methoxypropane 8: 3-[2,2-Bis(prop-2-ynyloxymethyl)propyloxy]prop-1-yne **2** (25 μmol, 5.9 mg), tetrahyaluronan azide **4** (75 μmol, 60 mg) and TBTA (1.8 μmol, 0.9 mg) was dissolved in dry, degassed methanol (0.01 M). A degassed aqueous solution (0.5 mL) of copper sulfate pentahydrate (2.5 μmol, 0.6 mg) was added. Sodium ascorbate (5 μmol, 1 mg) was given into the reaction mixture in one portion. The reaction was monitored by LCMS, and further ascorbate added until only trisubstituted product was detected. The solvent was removed under vacuum and small molecule impurities removed by size-exclusion chromatography (Sephadex G-10, H_2O). Purification by HPLC (C-18, isocratic 95:5 H_2O (+0.1%TFA)/MeCN (+0.1%TFA) for 12 min. to 50:50 in 20 min) and lyophilization gave the final product as a colorless powder (65.3 mg, 99%). ^{1}H NMR (600 MHz, D_2O): $\delta=8.18$ (s, 3H, triazole-H), 5.85 (d, $J=9.7$ Hz, 3H, I–H1), 4.59–4.54 (m, 9H), 4.42–4.38 (m, 4H), 4.05–3–98 (m, 11H), 3.83–3.78 (m, 14H), 3.75–3.72 (m, 16H), 3.66–3.61 (m, 6H), 3.56–3.50 (m, 12H), 3.38–3.31 (m, 10H), 1.97 (s, 9H, I-NHAc), 1.73 (s, 9H, III-NHAc), 0.76 (s, 3H, 2′-CH_3) ppm. ^{13}C NMR (151 MHz, D_2O): $\delta=$174.79, 174.00, 171.98, 170.94, 145.03, 123.97, 103.01, 102.68, 101.26, 86.21, 82.73, 82.22, 80.29, 78.63, 75.41, 75.11, 74.14, 73.77, 73.30, 72.50, 72.23, 72.13, 71.16, 68.35, 68.00, 60.60, 60.51, 54.29, 54.20, 40.00, 22.44, 21.84, 16.80 ppm. HRMS (ESI) calculated for $C_{98}H_{145}N_{15}O_{69}^-$: 1318.4171 Da $[M\text{-}2H^+]^{2-}$; found: 1318.4200 *m/z*.

Heptaicosa-sulfo tetrahyaluronan trimer (27 s-HA4 trimer): 1,3-[2-methyl-2-(2,3,4,6-tetra-*O*-sulfo-β-D–glucopyranuronyl-(1→3)-4,6-di-*O*-sulfo-β-D-2-acetamido-2-deoxyglucopyranosyl-(1→4)-2,3,4,6-tetra-*O*-sulfo-β-D–glucopyranuronyl-(1→3)-4,6-di-*O*-sulfo-β-D-2-acetamido-2-deoxyglucopyranosyl-(1,2,3-triazol-4-yl))methoxymethyl]-bis(2,3,4,6-tetra-*O*-sulfo-β-D–glucopyranuronyl-(1→3)-4,6-di-*O*-sulfo-β-D-2-acetamido-2-deoxyglucopyranosyl-(1→4)-2,3,4,6-tetra-*O*-sulfo-β-D–glucopyranuronyl-(1→3)-4,6-di-*O*-sulfo-β-D-2-acetamido-2-deoxyglucopyranosyl-(1,2,3-triazol-4-yl))methoxypropane 9: Tetrahyaluronan trimer **8** (18.8 μmol, 49.7 mg) underwent sulfation by SO_3·DMF complex (2 mmol, 323.2 mg) in dry DMF (0.024 M). After stirring overnight, additional sulfur trioxide complex (1 mmol, 159.2 mg) was added and stirred for another 2 hours. In the meantime, a sodium acetate (6.1 mmol, 500 mg) in ethanol (0.05 M) solution was prepared and cooled down in the fridge. The solution was added to the reaction mixture and the precipitate filtered off. The white solid was dissolved in and dialyzed against deionized water to give the final product (70%, 73.2 mg) after lyophilization. ^{1}H NMR (700 MHz, D_2O): $\delta=8.31$–8.28 (m, 3H, triazole-H), 6.15–6.06 (m, 3H, I–H1), 5.28–5.26 (m, 2H), 5.18–5.06 (m, 6H), 5.04–4.91 (m, 6H), 4.73–4.71 (m, 3H), 4.67–4.62 (m, 11H), 4.58–4.50 (m, 13H), 4.46–4.34 (m, 10H), 4.34–4.27 (m, 10H), 4.00–3.87 (m, 9H), 3.79–3.73 (m, 3H), 3.43–3.39 (m, 6H), 2.24–2.17 (m, 9H, I-NHAc), 1.95–1.87 (m, 9H, III-NHAc), 0.88 (s, 3H, 2′-CH_3) ppm. ^{13}C NMR (176 MHz, D_2O): $\delta=$174.93–174.32 (m), 144.33, 124.24, 101.33, 100.04, 99.45, 81.70, 78.67, 78.00, 77.49, 76.71, 75.61, 75.53, 73.64, 72.80, 72.64, 68.25, 68.19, 67.41, 67.16, 63.54, 60.63, 55.70, 54.55, 40.09, 22.88, 22.22, 16.80 ppm.

Tetrahyaluronan tetramer, (HA4 tetramer): 1,3-[2,2-bis(β-D–glucopyranuronyl-(1→3)-β-D-2-acetamido-2-deoxyglucopyranosyl-(1→4)-β-D–glucopyranuronyl-(1→3)-β-D-2-acetamido-2-deoxyglucopyranosyl-(1,2,3-triazol-4-yl))methoxymethyl]-bis(β-D–glucopyranuronyl-(1→3)-β-D-2-acetamido-2-deoxyglucopyranosyl-(1→4)-β-D–glucopyranuronyl-(1→3)-β-D-2-acetamido-2-deoxyglucopyranosyl-(1,2,3-triazol-4-yl))methoxypropane 10: A solution of copper sulfate pentahydrate in degassed water was added to the degassed methanolic (0.01 M) reaction mixture, that included tetrakis(2-propynyloxymethyl)methane **3** (25 μmol, 7.2 mg), tetrahyaluronan azide **4** (100 μmol, 80 mg) and TBTA (1.8 μmol, 0.9 mg). This was followed by addition of sodium ascorbate (5 μmol, 1 mg). The reaction was monitored via LCMS and sodium ascorbate added until all four alkyne residues of the tetravalent linker had undergone the cycloaddition reaction. The solvent was removed in vacuum and the crude mixture purified by size-exclusion chromatography (Sephadex G-10, H_2O) and by HPLC (C-18, isocratic 95:5 H_2O (+0.1%TFA) / MeCN (+0.1%TFA) for 12 min. to 50:50 in 20 min) to furnish **10** as a colorless solid (76.6 mg, 88%). ^{1}H NMR (500 MHz, D_2O): $\delta=8.15$ (s, 4H, triazole-H), 5.84 (d, $J=9.7$ Hz, 4H, I–H1), 4.59–4.55 (m, 10H), 4.52–4.50 (m, 7H), 4.41–4.37 (m, 4H), 4.04–3.97 (m, 11H), 3.90–3.86 (m, 6H), 3.83–3.78 (m, 11H), 3.75–3.71 (m, 14H), 3.63 (t, $J=9.1$ Hz, 1H), 3.57–3.55 (m, 8H), 3.50–3.48 (m, 6H), 3.39–3.28 (m, 14H), 1.97 (s, 12H, I-NHAc), 1.71 (s, 12H, III-NHAc) ppm. ^{13}C NMR (126 MHz, D_2O): $\delta=$174.97, 174.10, 172.11, 171.06, 144.27, 124.15, 103.13, 102.81, 101.39, 86.33, 82.86, 82.34, 80.34, 78.75, 75.54, 75.23, 74.27, 73.89, 73.43, 72.62, 72.25, 71.28, 68.47, 68.14, 63.56, 60.72, 54.41, 54.32, 44.74, 22.57, 21.95 ppm. HRMS (ESI) calculated for $C_{129}H_{190}N_{20}O_{92}^-$: 1746.0424 Da $[M\text{-}2H^+]^{2-}$; found: 1746.0458 *m/z*.

Hexatriaconta-sulfo tetrahyaluronan tetramer (36 s-HA4 tetramer): 1,3-[2,2-bis-(2,3,4,6-tetra-*O*-sulfo-β-D–glucopyranuronyl-(1→3)-4,6-di-*O*-sulfo-β-D-2-acetamido-2-deoxyglucopyranosyl-(1→4)-2,3,4,6-tetra-*O*-sulfo-β-D–glucopyranuronyl-(1→3)-4,6-di-*O*-sulfo-β-D-2-acetamido-2-deoxyglucopyranosyl-(1,2,3-triazol-4-yl))methoxymethyl]-bis(2,3,4,6-tetra-*O*-sulfo-β-D–glucopyranuronyl-(1→3)-4,6-di-*O*-sulfo-β-D-2-acetamido-2-deoxyglucopyranosyl-(1→4)-2,3,4,6-tetra-*O*-sulfo-β-D–glucopyranuronyl-(1→3)-4,6-di-*O*-sulfo-β-D-2-acetamido-2-deoxyglucopyranosyl-(1,2,3-triazol-4-yl))methoxypropane 11: Sulfur trioxide-DMF complex (2.45 mmol, 390 mg) was added to a solution of tetrahyaluronan tetramer **10** (17 μmol, 60 mg) in dry DMF (0.3 M). The mixture was stirred overnight and further SO_3·DMF (1.22 mmol, 195 mg) added in the morning. After two more hours, the product was precipitated by addition of cold ethanolic sodium acetate (7.4 mmol, 608 mg) solution (0.05 M). The colorless solid was filtered off and rinsed with cold ethanol. The final product (95.3 mg, 76%) was furnished through dissolving in and dialyzing against deionized water followed by freeze-drying. ^{1}H NMR (700 MHz, D_2O): $\delta=8.16$ (s, 4H, triazole-H), 6.00–5.86 (m, 4H, I–H1), 5.17–4.81 (m, 12H), 4.62–4.14 (m, 49H), 4.05–3.38 (m, 47H), 2.13–2.03 (m, 12H, I-NHAc), 1.83–1.74 (m, 12H, III-NHAc) ppm. ^{13}C NMR (126 MHz, D_2O): $\delta=176$ MHz, D_2O): $\delta=$174.80–173.85 (m), 144.69, 124.19, 102.06, 100.84, 99.36, 85.70, 81.56, 77.96, 77.46, 76.58, 75.52, 74.89, 73.63, 72.60, 68.07, 67.36, 67.13, 67.07, 63.57, 62.91, 54.93, 54.70, 46.84, 22.78, 21.90 ppm.

Acknowledgements

The work presented in this article was financially supported by the Deutsche Forschungsgemeinschaft (DFG SFB-TRR67 59307082, subprojects A6 and A8 and by the DFG-funded core facility Biosupramol. Open Access funding enabled and organized by Projekt DEAL.

Conflict of Interests

The authors declare no conflict of interest.

Data Availability Statement

The data that support the findings of this study are available in the supplementary material of this article.

Keywords: artificial proteoglycans · chemokine interleukin 8 (IL-8) · isothermal titration calorimetry (ITC) · multivalency · sulfated glycosaminoglycans (GAG)

[1] a) R. L. Jackson, S. J. Busch, A. D. Cardin, *Physiol. Rev.* **1991**, *71*, 481–539; b) G. Ruiz-Gómez, J. Salbach-Hirsch, J.-N. Dürig, L. Köhler, K. Balamurugan, S. Rother, S.-L. Heidig, S. Moeller, M. Schnabelrauch, G. Furesi, S. Pählig, P. M. Guillem-Gloria, C. Hofbauer, V. Hintze, M. T. Pisabarro, J. Rademann, L. C. Hofbauer, *Biomaterials* **2023**, *297*, 122105; c) S. D. Vallet, O. Clerc, S. Ricard-Blum, *J. Histochem. Cytochem.* **2021**, *69*, 93–104; d) J. Schiller, K. Lemmnitzer, J.-N. Dürig, J. Rademann, *Biol. Chem.* **2021**, *402*, 1375–1384.
[2] a) I. G. Colditz, M. A. Schneider, M. Pruenster, A. Rot, *Thromb. Haemostasis* **2007**, *97*, 688–693; b) G. S. V. Kuschert, F. Coulin, C. A. Power, A. E. I. Proudfoot, R. E. Hubbard, A. J. Hoogewerf, T. N. C. Wells, *Biochemistry* **1999**, *38*, 12959–12968.
[3] R. Derler, B. Gesslbauer, C. Weber, E. Strutzmann, I. Miller, A. Kungl, *Int. J. Mol. Sci.* **2017**, *18*, 2605.
[4] S. Misra, V. C. Hascall, R. R. Markwald, S. Ghatak, *Front. Immunol.* **2015**, *6*.
[5] C. I. Gama, L. C. Hsieh-Wilson, *Curr. Opin. Chem. Biol.* **2005**, *9*, 609–619.
[6] A. Pichert, S. A. Samsonov, S. Theisgen, L. Thomas, L. Baumann, J. Schiller, A. G. Beck-Sickinger, D. Huster, M. T. Pisabarro, *Glycobiology* **2011**, *22*, 134–145.
[7] S. Köhling, J. Blaszkiewicz, G. Ruiz-Gómez, M. I. Fernández-Bachiller, K. Lemmnitzer, N. Panitz, A. G. Beck-Sickinger, J. Schiller, M. T. Pisabarro, J. Rademann, *Chem. Sci.* **2019**, *10*, 866–878.
[8] K. Rajarathnam, C. M. Kay, I. Clark-Lewis, B. D. Sykes, in *Methods Enzymology, Vol. 287*, Academic Press, San Diego, **1997**, pp. 89–105.
[9] a) S. D. Burrows, M. L. Doyle, K. P. Murphy, S. G. Franklin, J. R. White, I. Brooks, D. E. McNulty, M. O. Scott, J. R. Knutson, D. Porter, P. R. Young, P. Hensley, *Biochemistry* **1994**, *33*, 12741–12745; b) E. F. Barter, M. J. Stone, *Biochemistry* **2012**, *51*, 1322–1331.
[10] a) V. Gross, R. Andreesen, H.-G. Leser, M. Ceska, E. Liehl, M. Lausen, E. H. Farthmann, J. Schölmrich, *Eur. J. Clin. Investig.* **1992**, *22*, 200–203; b) O. Kofanova, E. Henry, R. Aguilar Quesada, A. Bulla, H. Navarro Linares, P. Lescuyer, K. Shea, M. Stone, G. Tybring, C. Bellora, F. Betsou, *Clin. Chem. Lab. Med.* **2018**, *56*, 1054–1062.
[11] a) C. W. Frevert, M. G. Kinsella, C. Vathanaprida, R. B. Goodman, D. G. Baskin, A. Proudfoot, T. N. C. Wells, T. N. Wight, T. R. Martin, *Am. J. Respir. Cell Mol. Biol.* **2003**, *28*, 464–472; b) B. Goger, Y. Halden, A. Rek, R. Mösl, D. Pye, J. Gallagher, A. J. Kungl, *Biochemistry* **2002**, *41*, 1640–1646; c) A. J. Hoogewerf, G. S. V. Kuschert, A. E. I. Proudfoot, F. Borlat, I. Clark-Lewis, C. A. Power, T. N. C. Wells, *Biochemistry* **1997**, *36*, 13570–13578.
[12] K. Rajarathnam, U. R. Desai, *Front. Immunol.* **2020**, *11*.
[13] S. T. Das, L. Rajagopalan, A. Guerrero-Plata, J. Sai, A. Richmond, R. P. Garofalo, K. Rajarathnam, *PLoS One* **2010**, *5*.
[14] S. Köhling, G. Künze, K. Lemmnitzer, M. Bermudez, G. Wolber, J. Schiller, D. Huster, J. Rademann, *Chem. Eur. J.* **2016**, *22*, 5563–5574.
[15] a) P. R. B. Joseph, P. D. Mosier, U. R. Desai, K. Rajarathnam, *Biochem. J.* **2015**, *472*, 121–133; b) D. Schlorke, L. Thomas, S. A. Samsonov, D. Huster, J. Arnhold, A. Pichert, *Carbohydr. Res.* **2012**, *356*, 196–203.
[16] a) A. L. Jansma, J. P. Kirkpatrick, A. R. Hsu, T. M. Handel, D. Nietlispach, *J. Biol. Chem.* **2010**, *285*, 14424–14437; b) A. Penk, L. Baumann, D. Huster, S. A. Samsonov, *Glycobiology* **2019**, *29*, 715–725; c) J. J. Ziarek, C. T. Veldkamp, F. Zhang, N. J. Murray, G. A. Kartz, X. Liang, J. Su, J. E. Baker, R. J. Linhardt, B. F. Volkman, *J. Biol. Chem.* **2013**, *288*, 737–746.
[17] P. R. B. Joseph, K. M. Poluri, P. Gangavarapu, L. Rajagopalan, S. Raghuwanshi, R. M. Richardson, R. P. Garofalo, K. Rajarathnam, *Biophys. J.* **2013**, *105*, 1491–1501.
[18] a) J. Cavanagh, W. J. Fairbrother, A. G. Palmer, M. Rance, N. J. Skelton in *Protein NMR Spectroscopy* 2nd ed. (Eds.: J. Cavanagh, W. J. Fairbrother, A. G. Palmer, M. Rance, N. J. Skelton), Academic Press, Burlington, **2007**, p. 263; b) R. E. Hoffman, *Magn. Reson. Chem.* **2006**, *44*, 606–616.
[19] W. Lee, M. Tonelli, J. L. Markley, *Bioinformatics* **2014**, *31*, 1325–1327.
[20] a) S. Mori, C. Abeygunawardana, M. O. Johnson, P. C. M. Vanzijl, *J. Magn. Reson. Ser. B* **1995**, *108*, 94–98; b) A. J. Shaka, P. B. Barker, R. Freeman, *J. Magn. Reson.* **1985**, *64*, 547–552; c) V. Sklenar, M. Piotto, R. Leppik, V. Saudek, *J. Magn. Reson. Ser. A* **1993**, *102*, 241–245.

Manuscript received: August 23, 2023
Accepted manuscript online: November 27, 2023
Version of record online: January 15, 2024